SIMULATIONS STUDY OF REVERSE-TAPER ENHANCED HARMONIC LASING AT SXFEL

Weijie Fan, Yaozong Xiao, Zhangjiang laboratory, Shanghai, China
Chao Feng*, Kaiqing Zhang†, Shanghai Advanced Research Institute,
Chinese Academy of Sciences, Shanghai, China

Abstract

X-ray Free-electron lasers (XFELs) have been proven indispensable in scientific research, offering powerful tools in many scientific aspects. The self-amplified spontaneous Emission (SASE) mode is a fundamental mode at modern FEL facilities, known for its poor longitudinal coherence and spectral spikes. To address these limitations, harmonic lasing self-seeded (HLSS) technology has been promoted to enhance spectral performance and reduce spikes. The Shanghai Soft X-ray Free Electron Laser (SXFEL) facility, initially based on SASE mode, aims to achieve higher X-ray wavelengths through HLSS techniques. Here we show the simulation studies focusing on improving HLSS mode with reverse-tapered undulators to further enhance spectral performance.

INTRODUCTION

Free-electron lasers (FELs) have been developed for several decades to generate X-rays with extreme parameters, pushing towards shorter wavelengths. However, the achievable wavelength is always limited by various factors, including beam energy, undulator gap length, and undulator period length. To broaden the wavelength coverage of FELs, several schemes have been proposed, such as High Gain Harmonic Generation (HGHG) and Echo-Enabled Harmonic Generation (EEHG). A simple approach to extending photon coverage with a fixed beamline setup is the harmonic lasing technique, which involves a simple second-stage undulator resonating at the harmonics. The harmonic lasing self-seeded (HLSS) [5] [6] mode provides a straightforward method to extend the wavelength range. The Shanghai Soft X-ray Free Electron Laser (SXFEL) facility, which has a relatively low beam energy, primarily operates in the self-amplified spontaneous emission (SASE) [4] mode and externally seeding mode. It is crucial for providing soft X-ray FELs with shorter wavelengths to scientists at SXFEL; thus, the HLSS mode was promoted as a priority. The HLSS mode, employed at the external seeding beamline of SXFEL, takes advantage of gap-tunable undulators with different period lengths. This enables a degraded electron beam to generate harmonics with optimal efficiency. Furthermore, the use of reverse-tapered [1] [2] [3] undulators prevents further degradation of the electron beam, ensuring its quality for the second-stage radiation. This paper presents the simulated results of the reverse-tapered enhanced HLSS, and experimental validation is planned for the future.

* fengc@sari.ac.cn
† Zhangkq@sari.ac.cn

PRINCIPLE

Harmonic lasing in a high-gain Free-Electron Laser (FEL) refers to the amplification process where higher-order (typically odd-order) and fundamental harmonics mutually amplify each other in the exponential gain regime. In a typical FEL interaction, the electron beam will oscillate near the resonant wavelength

$$\lambda_h = \frac{\lambda_w \left(1 + K^2\right)}{2h\gamma^2} \quad h = 1, 3, 5 \ldots \tag{1}$$

where λ_w is the period length of an undulator, γ is the Lorentz factor and K the rms undulator parameter and can be described as

$$K = 0.934\lambda_w[cm]B_{rms}[T], \tag{2}$$

where B_{rms} is the magnetic strength of the undulator. For gap-tunable undulators, harmonic lasing is often prioritized over fundamental lasing. In this case, harmonic lasing can be achieved with undulators set to a higher K value. When switching to fundamental lasing, the K value should be reduced to K_{re}

$$K_{re}^2 = \frac{1 + K^2}{h} - 1. \tag{3}$$

Then we can derive the ratio between the gain length of the fundamental harmonic $L_g^{(1)}$ and the gain length of the higher harmonic $L_g^{(h)}$

$$\frac{L_g^{(1)}}{L_g^{(h)}} = \frac{h^{1/2} K A_{JJh}(K)}{K_{re} A_{JJl}(K_{re})} \tag{4}$$

where $A_{JJh}(K) = J_{(h-1)/2}\left(\frac{hK^2}{2\left(1+K^2\right)}\right) - J_{(h+1)/2}\left(\frac{hK^2}{2\left(1+K^2\right)}\right)$ is the coupling factor of Bessel function J_n for the nth harmonic.

The coherence length enhancement factor (or bandwidth reduction factor) depends on the saturation length in the HLSS mode compared to the SASE mode, which can be expressed as

$$R \simeq h\frac{\sqrt{L_w^{(1)} L_{sat,h}}}{L_{sat,1}} \tag{5}$$

where h is the harmonic number, $L_{sat,1}$ is the saturation length of the fundamental harmonic with smaller K, $L_w^{(1)}$ is the period length of the first stage undulator, $L_{sat,h}$ the saturation length of harmonic lasing. Equation (5) implies that increasing the undulator length of the first radiation section can reduce the radiation bandwidth to some extent.

Based on the analysis above, although increasing the length of the first stage can effectively reduce the final radiation bandwidth, in practical experiments, this always results in an increase in the energy spread of the electron beam in the first stage. This leads to suboptimal radiation performance in the second stage. Therefore, a reverse-taper undulator is introduced to suppress the energy spread growth of the electron beam in the first stage and increase the slippage length of FEL. Thus, the gain length will be increased and the bandwidth of the output FEL will be further reduced. In a reverse-taper undulator, the relationship between the fundamental bunching factor and the corresponding complex variable of energy modulation can be expressed as

$$|b_1|^2 \simeq |\beta\hat{z}|^2\hat{\eta}, \quad |b_p|^2 \simeq |\beta\hat{z}|\hat{\eta}, \tag{6}$$

where $\hat{z} = \frac{4\pi\rho z}{\lambda_u}$ (z is the coordinate along the undulator), β is the taper strength and can be expressed as $\beta = -\frac{\lambda_u}{4\pi\rho^2}\frac{K}{1+K^2}\frac{dK}{d\hat{z}}$, $\hat{\eta}$ is the normalized FEL radiation power. Besides, for the nonlinear harmonic radiation process, the following expression can be obtained

$$b_n \propto \left(\frac{P_0}{9\rho P_E}\right)^{n/2}, \tag{7}$$

where b_n is the bunching factor for nth harmonic, P_0 is the initial power of laser, P_E is the initial power of electron beam. Therefore, the bunching factor of the linear stage for the high-gain FEL can be written as

$$|b_n|^2 \propto \left(\frac{P_0}{9P_E}\right)^{(n-1)/2} \frac{(\rho_n)^{n/2}}{(\rho_1)^{1/2}}|\beta\hat{z}|^2\hat{\eta} = A|\beta\hat{z}|^2\hat{\eta}, \tag{8}$$

where $A = \left(\frac{P_0}{9P_E}\right)^{(n-1)/2}\frac{(\rho_n)^{n/2}}{(\rho_1)^{1/2}}$, is a constant in FEL radiation. Equations (6) and (8) show that b_n is proportional to β for nth harmonic, and the amplitude of the corresponding energy modulation is proportional to $\sqrt{\beta}$. In non-taper undulators, $|b_1^2|$ is of the same order of magnitude as the FEL normalized energy $\hat{\eta}$. As the distance z in the undulator increases, FEL power together with the energy modulation amplitude also increase rapidly, which indicates that the quality of the electron beam will gradually deteriorate and can hardly radiate in the second stage.

RESULTS

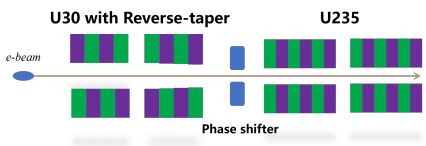

Figure 1: Conceptual scheme of the HLSS mode at SXFEL.

Here, we perform parameter optimizations and provide the optimal HLSS mode performance utilizing the SXFEL parameters. The beamline configuration is depicted in Fig. 1. The upstream electron beam for linac will first enter the first stage undulator and resonate at 5.91 nm, where reverse-tapered undulators are present to suppress the energy spread growth. After entering the second-stage undulator, the radiated electron beam will resonate at 2.956 nm and reach saturation. Table 1 lists the parameters of the electron beam and undulators. Simulations are carried out by the 3D time-dependent FEL code GENESIS [7].

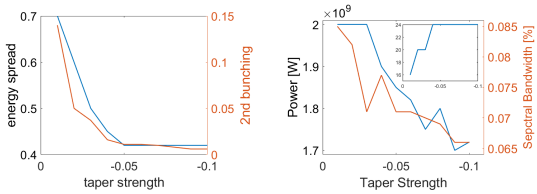

Figure 2: Left is bunching factor of the 2nd harmonic and energy spread at the exit of the first stage radiator versus the strength of the reverse-taper. Right is bandwidth, power and saturation length of the final FEL radiation versus the strength of the reverse-taper.

The results of changing the strength of the reverse-taper undulator are presented in Fig. 2. Left illustrates the changes in beam quality at the exit of the reverse-taper undulator after altering its strength. With an increase in the reverse-taper strength, it can be observed that the FEL radiation in the SASE mode is significantly suppressed, and the energy spread of the beam gradually decreases. However, the bunching factor at the entrance of the second stage also correspondingly decreases. When the reverse-taper strength exceeds 0.05, the reduction in beam energy spread becomes less noticeable. Further increasing the strength would eliminate the initial bunching factor.

It is evident that as the strength of the reverse-taper undulator increases, as shown in Fig. 3, the gain length and saturation length in the HLSS mode also increase from 16 m to 24 m, and the final FEL radiation bandwidth continues

Table 1: Main parameters of the simulation

Parameters	**Value**	**Unit**
Electron Beam		
Beam energy	1410	MeV
Energy Spread	0.013%	-
Peak Current	800	A
Bunch length (FWHM)	500	fs
Normalized Emittance	1.5	mm·rad
Undulator Parameters (1st stage / 2nd stage)		
Period length	0.03/0.0235	m
Resonate wavelength	5.91/2.956	nm
Period number	100/126	-
Total length	18/18	m

to decrease. This is consistent with theories above. However, when the reverse-taper undulator strength increases to around 0.1, the saturation length no longer increases, but the FEL radiation still decreases. Therefore, we choose a reverse-taper strength of 0.05 as the optimal value, where the bandwidth has already significantly narrowed, and the radiation power is not relatively low, ensuring that the final FEL spectrum intensity is not adversely affected.

From these figures, it can be seen that although the FEL spectral bandwidth is relatively narrow, about 0.065%, when the reverse-taper is set relatively early, the peak radiation power of the FEL is also relatively low, only about 0.5 GW. Whereas, when the reverse-taper is set at the end of the third undulator, i.e., at 12 m, the FEL radiation spectral bandwidth is also relatively narrow, about 0.6%, and the peak power can reach a relatively high level, about 1 GW. When the reverse-taper position is set further back, although the FEL power increases, the radiation bandwidth also broadens. Therefore, we choose to set the reverse-taper starting from the end of the third undulator.

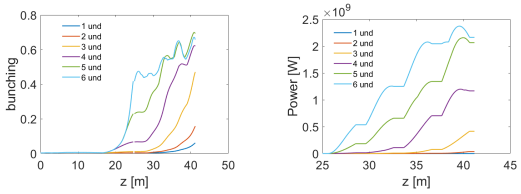

Figure 3: Left is bunching factor evolution along the undulator versus the location of the reverse-taper. Right is evolution of the final FEL power along the undulator versus the location of the reverse-taper.

Based on the optimization results, FEL simulations were performed with a reverse-taper strength of 0.05 and a starting position at the end of the third undulator. To compare with the final output results of the SASE mode, the same radiation section undulator was used for the simulation. This undulator consists of 8 sections with a period of 0.0235 m for SASE radiation, allowing it to saturate at 32 m. To further illustrate the performance of the reverse-taper technique, multi-shot simulations were carried out based on this. Fig. 4 shows the results of the multi-shot GENESIS simulations for the regular SASE mode and the reverse-taper enhanced HLSS mode, with 500 shots conducted. Radiation bandwidth plots for both modes. It can be seen that the bandwidth of the SASE mode is approximately 0.075%, while the bandwidth of the enhanced HLSS mode is approximately 0.06%, resulting in a ratio of about 1.2. According to equation 5, the theoretical bandwidth ratio between the SASE mode and the HLSS mode is approximately 1.2 to 1.8. However, the simulations did not show such good results. Fig. 4 shows the average power of the two modes. The enhanced HLSS mode has an average power of 0.5 GW, which is lower than the 0.8 GW of the traditional SASE mode. However, considering both the bandwidth and energy, the spectral brilliance of the two modes is comparable, which aligns with the previous theoretical comparison. Furthermore, we conducted a stabil-

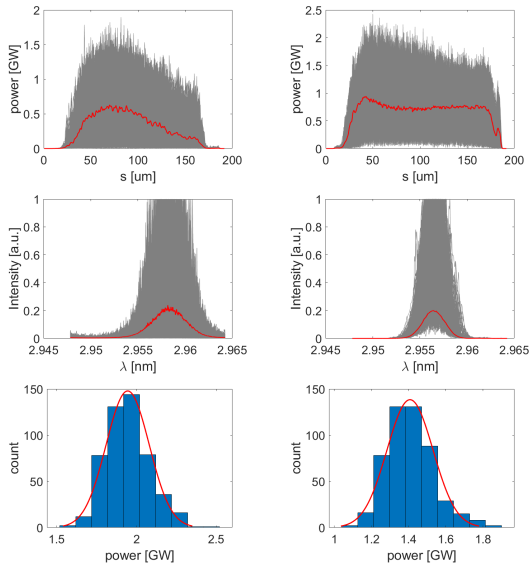

Figure 4: Top left: Bandwidth of the SASE mode. Top right: Bandwidth of the reverse-taper enhanced HLSS. Middle left: Power profiles of the SASE mode. Middle right: Power profiles of the reverse-taper enhanced HLSS. Bottom left: Power distribution of the SASE mode. Bottom right: Power distribution of the reverse-taper enhanced HLSS.

ity analysis based on multi-shot simulations. Fig. 4 shows the energy distribution plots for the two modes. In the SASE mode, the stability of the output FEL power is about 27%, while the stability of the enhanced HLSS mode is about 21%. Although the HLSS mode performs slightly better numerically, both modes exhibit significant fluctuations, which are attributed to the inherent noise of the electron beam. The solution proposed in this paper cannot completely address this issue.

CONCLUSION

This paper shows the simulation results of the HLSS mode at SXFEL. Simulation results show that the reverse-taper enhanced HLSS can significantly improve the performance of the traditional HLSS. Current simulations show limited improvement of the reverse-taper undulators. Thus, further investigations are underway to optimize the coherence of the reverse-taper enhance HLSS. Simulations results above provide valuable insights for future experimental implementation of the reverse-taper enhanced HLSS at SXFEL, paving the way for generating highly coherent for advanced scientific applications.

ACKNOWLEDGEMENTS

This work is supported by National Natural Science Foundation of China (12105347 and 12275340).

REFERENCES

[1] Lutman, Alberto A., et al. "Polarization control in an X-ray free-electron laser." Nature photonics 10.7 (2016): 468-472.

[2] Zhang, Kaiqing, Tao Liu, and Chao Feng. "Reverse taper enhanced harmonic lasing for seeding an X-ray free-electron laser." Nuclear Instruments and Methods in Physics Research Section A: Accelerators, Spectrometers, Detectors and Associated Equipment 988 (2021): 164931.

[3] Zhang, Kaiqing, et al. "Extending the photon energy coverage of a seeded free-electron laser via reverse taper enhanced harmonic cascade." Photonics. Vol. 8. No. 2. MDPI, 2021.

[4] Emma, Paul, et al. "First lasing and operation of an ångstrom-wavelength free-electron laser." nature photonics 4.9 (2010): 641-647.

[5] McNeil, B. W. J., et al. "Harmonic lasing in a free-electron-laser amplifier." Physical review letters 96.8 (2006): 084801.

[6] Nam, Inhyuk, et al. "Soft X-ray harmonic lasing self-seeded free electron laser at Pohang Accelerator Laboratory X-ray free electron laser." Applied Physics Letters 112.21 (2018).

[7] Reiche, Sven. "GENESIS 1.3: a fully 3D time-dependent FEL simulation code." Nuclear Instruments and Methods in Physics Research Section A: Accelerators, Spectrometers, Detectors and Associated Equipment 429.1-3 (1999): 243-248.